

UNCLASSIFIED

AD NUMBER

ADB190676

NEW LIMITATION CHANGE

TO

**Approved for public release, distribution
unlimited**

FROM

**Distribution authorized to U.S. Gov't.
agencies and their contractors; Foreign
Government Information; JUN 1994. Other
requests shall be referred to DSTO
Aeronautical and Maritime Research Lab.,
Melbourne, Australia.**

AUTHORITY

DODA ltr, 15 Mar 1995

THIS PAGE IS UNCLASSIFIED

AD-B190 676



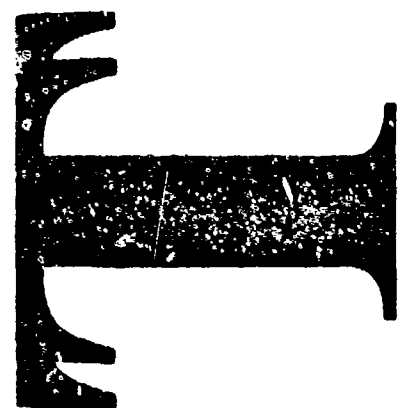
(1)

AR-008-920

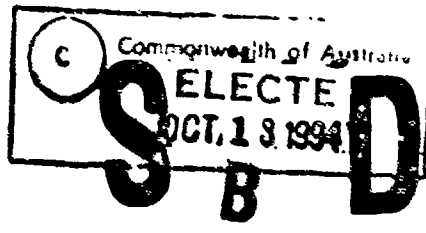
DSTO-TR-0002

Ultraviolet Emission from Rocket
Motor Plumes

David Kilpin



APPROVED
FOR PUBLIC RELEASE



Ultraviolet Emission from Rocket Motor Plumes

David Kilpin

DSTO Technical Report
DSTO-TR-0002

Abstract

Atmospheric limitations on the spectral region of the ultraviolet appropriate for detection of emissions from rocket motor plumes are considered. Origins of ultraviolet emission as spectral continua, bands and lines from the rocket motor exhaust flow and its atmospheric interaction are discussed. The contrast of infrared emissions arising mostly from major products and processes with ultraviolet emissions often resulting from trace constituents and minor pathways, indicates the more detailed knowledge of the rocket motor system required for modelling and prediction of ultraviolet signatures.

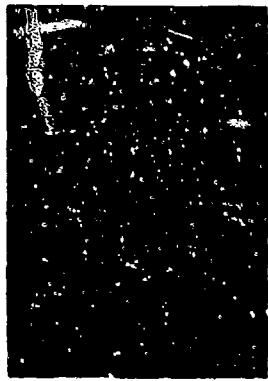
DEPARTMENT OF DEFENCE
DSTO AERONAUTICAL AND MARITIME RESEARCH LABORATORY

Published by

DSTO Aeronautical and Maritime Research Laboratory
GPO Box 4331
Melbourne Victoria 3001 Australia

Telephone: (03) 626 8111
Fax: (03) 626 6999
© Commonwealth of Australia 1994
AR No. 008-~~600~~ Q20

Author



D. Kilpin

David Kilpin joined the Department of Supply as a Defence Science Cadet in 1960. After completing his Chemistry degree at the University of WA he commenced upper atmosphere and combustion studies in Chemistry and Physics Division at Salisbury. He has since worked mainly in areas related to propellant combustion, with flash photolysis, shock tube, and windowed vessel techniques. More recently he has been involved in thermal imaging and rocket motor plume signatures."

Accession No.	
DTI3 JFAAI	<input checked="" type="checkbox"/>
DTI3 TAS	<input type="checkbox"/>
Other	<input type="checkbox"/>
JULY 1981	
BY _____	
Classification _____	
Analyst _____ Date _____	
Editor _____ Date _____	
Dist	Specialist
R-1	

Contents

1. INTRODUCTION 1
2. ATMOSPHERIC TRANSMISSION AND AMBIENT BACKGROUND 2
 - 2.1 *Defining the region and subregions* 2
 - 2.2 *Factors affecting transmission* 2
 - 2.2.1 *Ozone* 2
 - 2.2.2 *Oxygen* 6
 - 2.2.3 *Aerosols and particulates* 7
 - 2.3 *Regions of transmission* 7
 - 2.4 *Absorption detection* 8
 - 2.5 *UV transmission window* 8
3. MOTOR EMISSION 9
4. SUMMARY 13
5. REFERENCES 13

Ultraviolet Emission from Rocket Motor Plumes

1. Introduction

Rocket motor and aircraft engine plume emissions are logically thought of as strong infrared emitters because of their high temperatures. Their strong infrared emissions in clear atmospheric windows permits convenient discrimination against ambient backgrounds for detection purposes. However the lower intensity ultraviolet emissions combined with the lower ambient backgrounds in the ultraviolet region and acceptable atmospheric transmission at some points, together with simple, efficient and sensitive detectors, make that spectral region also suitable. Operational military detection systems such as the Loral AAR-47 have been described [1].

The detectability of motor emission at a particular wavelength is dependent on the intensity of that emission, the transmission of the atmosphere between the emitter and the detector, and the strength of the background signal. Variations of these parameters with wavelength in the ultraviolet results, in most cases, in only a narrow waveband region where efficient detection is possible. Unusual circumstances, such as intense line emission or satellite detection of high altitude emitters, may permit operation outside this 250 to 300 nm region. However for most cases of near horizontal paths through sea level or low altitude atmospheres, motor plume detection is restricted to the 260 to 290 nm region.

Atmospheric transmission and ambient radiation background predominantly determine the spectral region in which emissions can be detected and will be considered first. Sources of plume emission in the accessible region will then be discussed.

2. Atmospheric Transmission and Ambient Background

2.1 Defining the region and subregions

Ultraviolet radiation is usually defined as electromagnetic radiation of wavelengths between 4 and 400 nanometres. It can be subdivided into further regions of vacuum ultraviolet, encompassing the extreme ultraviolet from 4 to 100 nm and far ultraviolet from 100 to 200 nm, the middle ultraviolet from 200 to 300 nm and the near ultraviolet from 300 and 400 nm [2-4]. Wavelengths from 230 to 290 nm are frequently referred to as the solar blind ultraviolet, SBUV. Ultraviolet environmental effects on biological or physical systems are often considered for the ranges LVA, 400 to 315 nm, UVB, 315 to 280 nm, and UVC, <280 nm. In this report the region 200 to 400 nm will be considered and ambiguity avoided by referring to positions or regions by wavelengths.

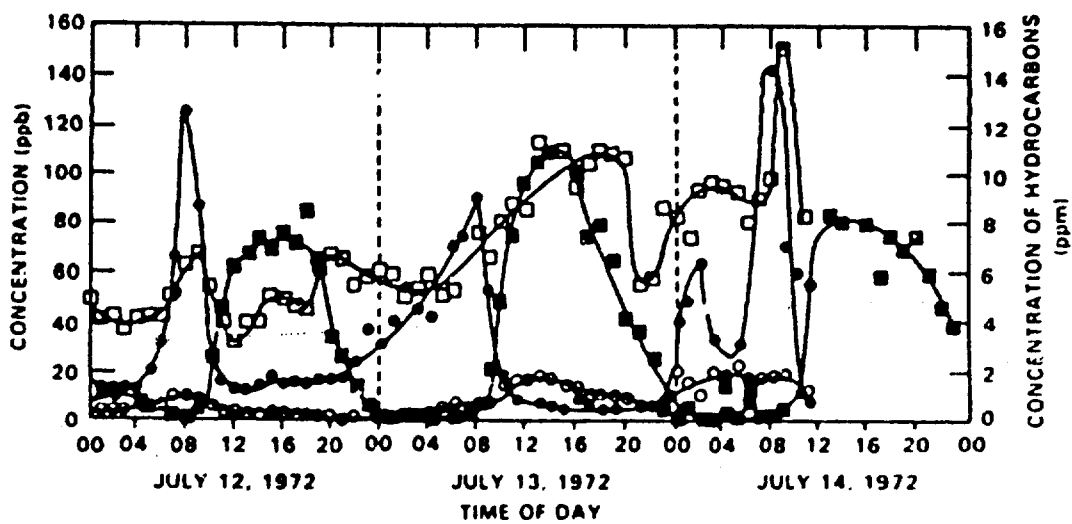
2.2 Factors affecting transmission

Transmission through a horizontal sea level atmospheric path for standard conditions is described in detail in several references [5-8]. At the long wavelength edge of the ultraviolet at 380-400 nm there is virtually no molecular absorption, with transmission being limited by molecular and particulate scattering, but capable of over 90% for paths of tens of kilometres. At shorter wavelengths of around 200 nm the uniform oxygen content limits transmission to 50%, for a path length of 15 metres, although scattering losses are greater here than at 400 nm. Intermediate wavelengths may be attenuated predominantly by either the variable particulate levels or the variable ozone content, whose absorption band is centred near 255 nm. Ozone concentrations vary with location and show regular temporal variations over diurnal and seasonal periods. The major effect of these ozone variations is to shift the short wavelength edge of the ultraviolet window near 270 nm.

2.2.1 Ozone

Sea level ozone concentrations may vary from 1 to 100 ppb [9-17]. This may therefore change the transmission of the atmosphere at ozone's absorption maximum at 255 nm (where the decadic base absorption coefficient is 132 cm^{-1}) from 97% to 22% over a one kilometre path or at 280 nm (where the absorption coefficient is 43 cm^{-1} [2]) from 99% to 61%. Typical urban midday concentrations of 30 ppb can fall to one to several ppb at midnight and then build up again next day via many processes in the sunlight irradiated polluted atmosphere. Concentrations of over 100 ppb are apparent in figure 1 [9] for London for three days of 1972. Anthropogenic emissions of ozone generating species modify the natural system of generation and vertical transport and surface destruction of ozone. In remote unpolluted environments there is a lower surface level, about

13 ppb for the Amazonian rain forest [15], but a similar diurnal variation. Surface ozone concentrations in Germany show average levels of about 30 ppb and annual cycles with winter minima and spring or summer maxima of about 1:2 ratio [16]. These variations are connected with temperature and solar radiation changes and anthropogenic emissions. Nighttime winter remote wilderness transmission is considerably higher than daytime summer urban, perhaps increasing 260 nm transmission over 1 km from 24% to 97%, or shifting the wavelength edge for 90% transmission over 4.6 kilometres from 307 nm to 268 nm.

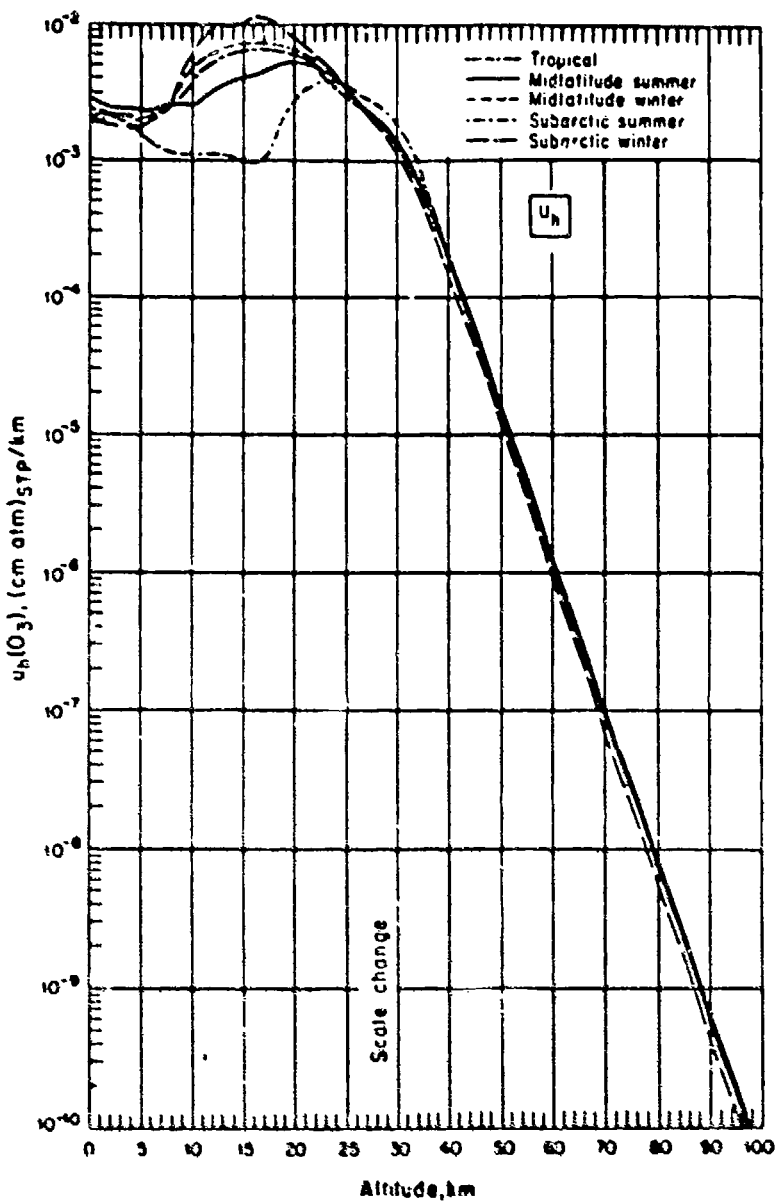


Diurnal variations of air pollutants measured in London from July 12 to July 14, 1972.
 ■, Ozone ppb; ●, nitric oxide, ppb; □, nitrogen dioxide, ppb. ○, hydrocarbons, ppm. From Derwent and Steward.

Figure 1: Diurnal variations of air pollutants

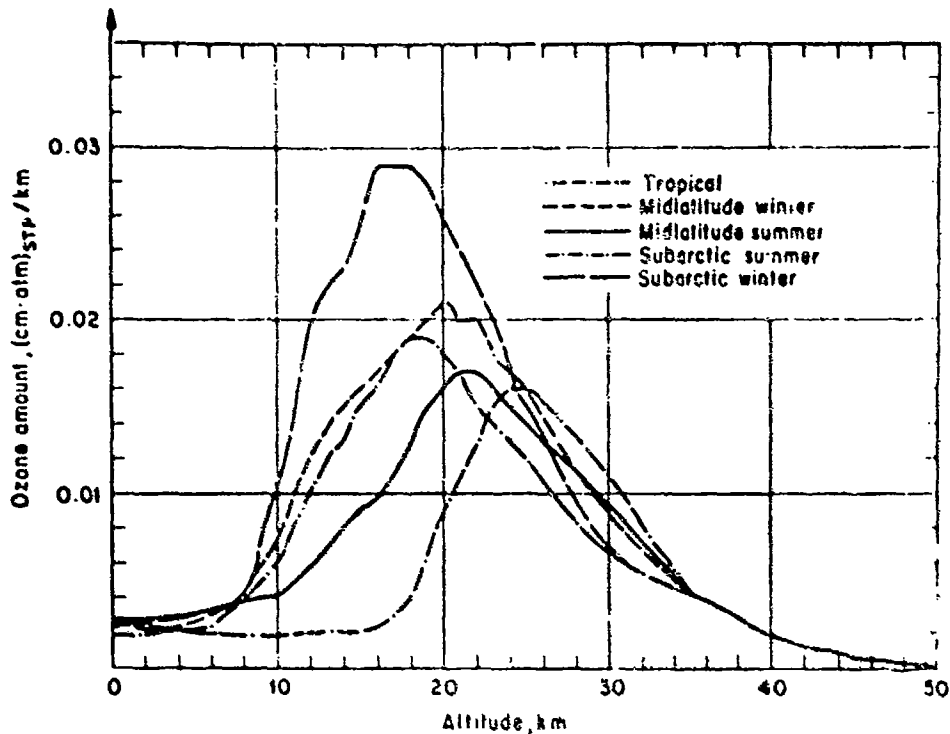
Vertical ultraviolet transmission over the 220 to 300 nm range depends on both path length and source and detector altitudes because of variations of ozone concentrations with height. Maximum concentrations occur at altitudes of up to 35 kilometres where the volume fraction of about 10 ppm combined with the pressure of 0.01 atmospheres results in about four times the ground level density (figures 2 (logarithmically scaled) and 3 (linearly scaled)[18]). Formation of ozone above this level by solar photolysis of oxygen is normally balanced by the downwards transport of ozone to levels where it undergoes destructive gaseous and surface reactions. This vertical distribution of ozone results in 80% upwards transmission of wavelengths of 290 nm from above 40 kilometres, but strong attenuation of similar wavelengths from ground level. Kolb et al (figure 4 [19]) show that even the weak wing of ozone absorption at 310 nm, where the absorption coefficient is 1, reduces vertical spacewards transmission to 30% from 10 kilometres, whereas horizontal ground level transmission is 79% over 50 kilometres at 20 ppb.

Best Available Copy



Equivalent sea-level path length of ozone as a function of altitude for horizontal atmospheric paths.

Figure 2: Logarithmic plot of ozone vs altitude



Equivalent sea-level path length for ozone (0.25 to 0.75 μm) as a function of altitude for horizontal atmospheric paths.

Figure 3: Linear plot of ozone vs altitude

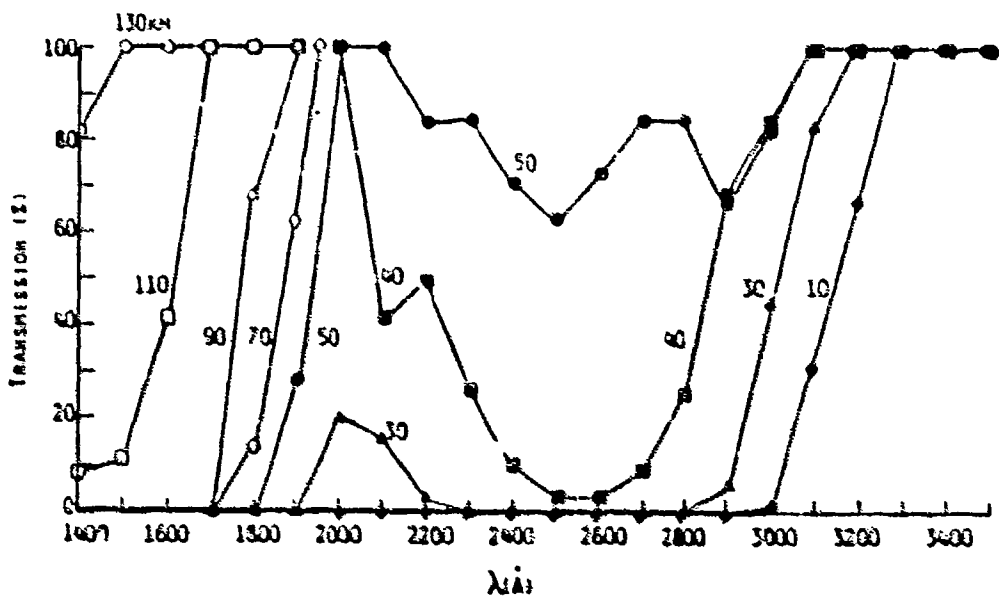
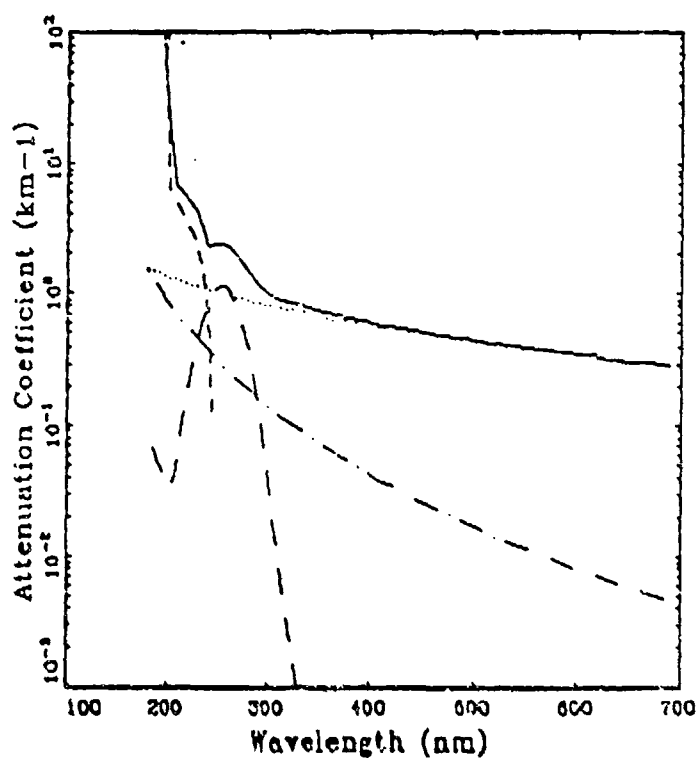


Figure 4: Ultraviolet radiation transmission to open space for a view angle 30° to the zenith.

2.2.2 Oxygen

At wavelengths shorter than the long wavelength ozone edge not only does molecular Rayleigh scattering and particulate scattering increase, but absorption by the forbidden Herzberg I bands and adjoining photodissociation continuum of molecular oxygen dominates [20,21]. Although the oscillator strength of the whole Herzberg system is only about 10^{-7} [20], this still reduces transmittance over a one kilometre horizontal path at 280 nm to 80% [6-8]. At shorter wavelengths the absorption increases to become the dominant attenuator at wavelengths below 220 nm (figure 5 [5]). At 220 nm molecular oxygen absorption over one kilometre reduces transmission to only 4% even if no molecular or particulate scattering attenuation occurred.

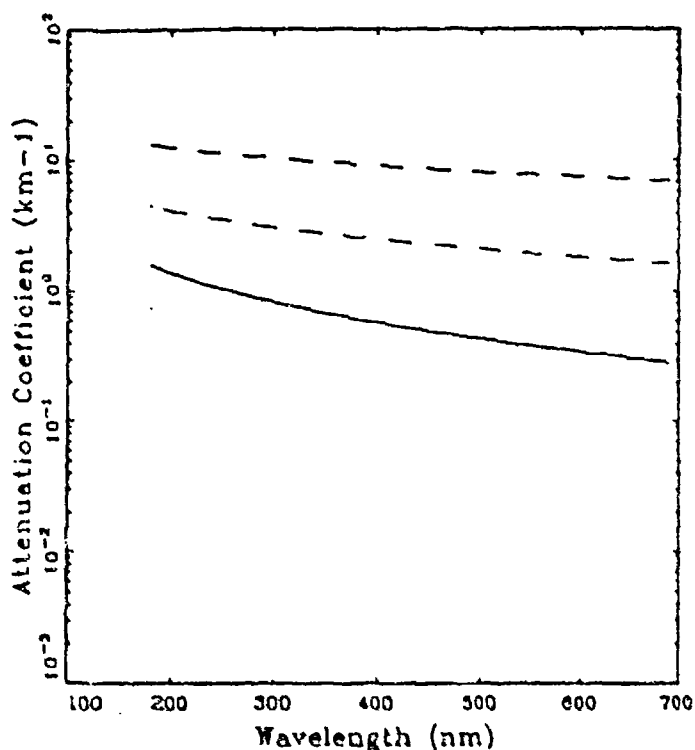


Attenuation calculations for standard conditions at sea level for an assumed visibility of 10 km. The total attenuation coefficient is given by the solid line, the aerosol attenuation by the dotted line, the molecular scattering attenuation by the dashed and dotted line, the ozone and oxygen attenuations by the long and short dashed lines, respectively.

Figure 5: Attenuation vs wavelength at 10 km visibility.

2.2.3 Aerosols and particulates

Aerosol effects on the clarity of the atmosphere are less spectrally selective than absorption, but more variable, and markedly limit atmospheric transmission. Scattering of radiation by the predominantly aqueous droplets and dust particulates increases with decrease of wavelength. The magnitude of the overall attenuation at a particular wavelength is dependant on the number and size distribution of the aerosols and their refractive indices. Slowly decreasing transmission with decrease of wavelength is shown for differing values of visibility in figure 6 [5]. This atmospheric clarity essentially determines the overall transmission at longer wavelengths than the ozone absorption band.



Model aerosol attenuation coefficients as a function of wavelength for different values of visibility V . The dotted line corresponds to $V = 50 \text{ km}$, the solid line to $V = 10 \text{ km}$, the dashed and dotted line to $V = 2 \text{ km}$, and the dashed line to a V of 0.5 km .

Figure 6: Aerosol attenuation vs wavelength.

2.3 Regions of transmission

The factors considered above combine to limit the ultraviolet transmission by the atmosphere over paths of a few kilometres or more to wavelengths of longer than about 270 nm. For low ozone levels, shorter paths, clear atmospheres and very bright sources, shorter wavelengths may be appropriate.

Longer wavelengths in the ultraviolet (300 to 400 nm) are usually of less interest, particularly for daytime applications, because of the increasing background radiation arising from the solar spectrum. The solar spectrum incident above the atmosphere approximates that of a blackbody near 6000K with a maximum near 500 nm. About 10% of the total energy is in the ultraviolet, with only 0.1% at wavelengths below 200 nm. The approximate 4:1 ratio of 400 nm to 300 nm fluxes above the atmosphere is severely altered by absorption and scattering to result in a 100:1 ratio at the surface [2]. This sharp falloff of direct sunlight and diffuse skylight with shorter wavelengths in the ultraviolet terminates totally at about 290 nm, due primarily to ozone absorption. Ultraviolet fluxes vary with solar altitude to midday maxima for both sun and sky origins. Seasonal variations also occur with maxima in summer. Reflection of the incident ultraviolet flux from natural and other surfaces results in a spatially and temporally variable background in the 300 to 400 nm region. Although narrow bandwidth spectral regions at the lower end of that range will have quite low background levels, best detectability of ultraviolet emissions will generally be beyond that clutter, before the atmospheric absorption attenuation, in the region 270 to 290 nm.

2.4 Absorption detection

Background daylight sky radiance has been used as a source against which the absorption of sulphur dioxide from a power plant stack plume at 318 nm can be observed with an ultraviolet video imaging system [22]. Similar 306 nm imaging of plume hydroxyl absorption against a daylight background might be possible with a differential dual band system to prevent false alarms of birdlike broadband spectral absorbers. However, the low hydroxyl concentration would probably result in poor sensitivity compared with emissive detection.

2.5 UV transmission window

For daylight situations the ultraviolet atmospheric window for kilometre scale horizontal pathlengths is limited to the region around 270 to 290 nm by the absorption of ozone at shorter wavelengths and the solar radiation background at longer wavelengths. Shorter wavelengths will be somewhat better transmitted at night and for clearer visibilities. The detectability of longer wavelength emissions would be greatly enhanced at night when there is no solar radiation background or thermal background emission. Daylight operation at some longer wavelengths can be enhanced for narrow band features by spectral filtering to minimise the background. However general operation is only possible in the 270 to 290 nm region and even there atmospheric attenuation can be severe in rain, clouds or fog.

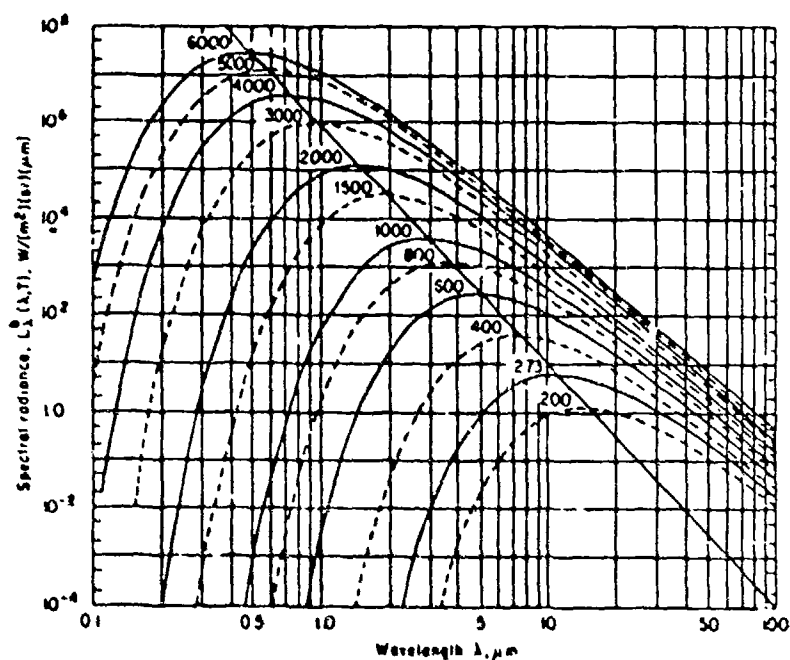
3. Motor Emission

Flames and rocket motor plumes radiate strongly in the infrared region because they are high temperature sources and blackbody emission results in peak spectral radiance at $2898 \mu\text{mK}$ wavelength-temperature product (figure 7 [18]). Even at 1000K there is a strong emission peak near $3\mu\text{m}$ and substantial longer wavelength emission both as a continuum from particulates and/or from molecular bands of combustion product gases. The rapid fall off of the Planck blackbody spectral radiance at shorter wavelengths results in very low fractions of the total energy in the ultraviolet unless very high temperatures are attained. This low level of ultraviolet emission is employed in atomic absorption analysis where the absorption of traces of elements aspirated into a flame is easily detected against a low background. Even at high temperatures ultraviolet emission is usually far less efficient than infrared emission because none of the major molecular combustion products have strong emission spectra in the ultraviolet, compared with carbon dioxide, carbon monoxide and water in the infrared. Ultraviolet emission therefore depends on either particulate blackbody emission or line or band emission from atomic and transient or low level radical or molecular species. It is consequently not only weaker but also more dependent on chemical composition and contributions from trace components. Apparently minor variations in propellant composition or impurity levels or component construction can result in major differences in ultraviolet outputs.

Rocket motor combustion of hydrocarbon propellants produces carbon dioxide and water as end products, with carbon monoxide as both an intermediate and end product, and many other species such as hydroxyl (OH), hydroperoxyl (HO_2) and atomic hydrogen and oxygen as intermediate reactants. Propellants containing ammonium perchlorate yield hydrogen chloride as an end product with some atomic chlorine as a reactive intermediate. A rich assortment of diatomic and polyatomic species arising from the component C, H, N, O and Cl atoms is also involved. In addition to these are the products from other additives, either as their primary decomposition fragments, or after oxidation or further reaction. While most of these reactants are in thermal equilibrium with their immediate surroundings, some result from chemical reactions which impart excess energy which is subsequently radiated as chemiluminescence from non-thermally equilibrated species. This complex mixture can then mix turbulently with cooler nitrogen and reactive oxygen to form an afterburning plume, from which ultraviolet emission can originate via many routes.

Hydrocarbon flames and rocket motor afterburning plumes do have some characteristic ultraviolet features [22-26]. Hydroxyl emission from the (1,0) and (0,0) bands at 281 and 306 nm is almost universal, as is the "blue flame" chemiluminescence from the atomic oxygen - carbon monoxide reaction. These emissions can overlie a blackbody continuum to give false indications of temperatures from wavelength intensity ratios. At longer wavelengths in the near ultraviolet bands from CN at 388 nm, CH at 387 nm and NH at 336 nm [23] may be present. An ultraviolet spectrum of a Saturn V (oxygen/kerosene) rocket shows a typical continuum due to the 1% of solid carbon particles in the exhaust plume with strong fall off of intensity from 400 to 280 nm [27]. The

"absorption" band at 300 nm, there incorrectly ascribed to ozone, is more likely due to a gap between emission bands of hydroxyl near 281 and 306 nm. Solid propellant rocket plumes studied by Keefer et al [28] showed hydroxyl emission to be the most consistently observed feature of the ultraviolet together with a 250 to 300 nm continuum whose intensity increased rapidly with wavelength, on which bands due to NO (many bands eg (0.6) of its β system at 289 nm and (0.4) of its γ system at 272 nm), PbO (287, 340 and 349 nm) and CHO (several, strongest at 330 nm) were also apparent.



Spectral radiance $L_*(\lambda, T)$ of a blackbody at the temperature in kelvins shown on each curve. The diagonal line intersecting each curve at its maximum shows Wien's displacement law. Subdivisions of the ordinate scale are at 2 and 5. (Adapted by permission from Valley (1985).)

Figure 7: Blackbody spectral radiance.

Processes contributing to ultraviolet emission from rocket motor plumes have been considered in several reports, both qualitatively [19,26], and quantitatively as part of plume prediction codes [29,30]. Continuum radiation originates either as particulate scattering of solar radiation, or chemiluminescence or greybody thermal emission from specific particulates such as alumina or zirconia or carbon, or broad chemiluminescence from the atomic oxygen/carbon monoxide reaction [31]. Transient or stable molecular species emit radiation as characteristic lines or bands, with hydroxyl and nitric oxide the major contributors, and carbon monoxide generally of minor importance.

Thermal emission from hot condensates is often the major continuum radiation apparent. Alumina, boria, zirconia and carbon particulates may be close to or far from thermal equilibrium with the gaseous plume, but will radiate some form of spectral continuum. Emissivity variations with surface purity may mean that strict greybody behaviour is not followed. Computations involving particle size distributions and refractive index values required for absorption cross sections modifying blackbody particulate emission yield estimates of these continua [29]. Chemiluminescence arises from nonthermally equilibrated reaction products. For the excited carbon dioxide from the reaction of atomic oxygen with carbon monoxide it is observed as a broad band centred at about 350 nm, but with substantial emission in the 250 to 300 nm range at high temperatures (figure 8 [19], [31]). Scattering of skylight and sunlight by the particulates will add to the pure emission continuum. Some or all of these factors are incorporated in the predictive codes.

Molecular emission is usually dominated by the strong 306 nm and weaker 281 nm hydroxyl bands [19, 28, 30, 32, 33]. While most of the thermally equilibrated hydroxyl results from the $H + O_2$, $O + H_2$ and $O + H + M$ reactions, emission is thought to result mostly from chemiluminescence from the electronically excited OH from $H + OH + OH$ or perhaps the $CH + O_2$ reaction [19, 30]. Thermal emission from the OH, CO and NO can be calculated from the equilibrium plume data from complex systems incorporating reactions such as those listed in reference 34. One of the few ultraviolet rocket plume spectra published in the open literature (figure 9 [33]) shows the strong hydroxyl (0-0) band and the (0-1), (0-2), (0-3) and (0-4) nitric oxide γ bands. Hydroxyl emission is usually the only molecular emission which it is essential to consider, although some exotic propellant compositions may produce strong emitters. Different criteria apply at very high altitudes where short wavelengths near 230 nm are transmitted and substantial motor plume continuum and vehicle shock CO Cameron band emissions are observed [35].

While atomic line emission is rarely considered as a source of ultraviolet since common propellant components contain no strongly emitting elements, intense resonance or other strong line emission is possible from low concentrations of particular elements. These elements may be present as burning rate modifiers or fillers in insulants, liners or nozzle components. Antimony at 253 nm, tin at 284 nm, magnesium at 285 nm and silicon at 288 nm may all arise from insulant and propellant additives, while bismuth at 307 nm, copper at 325 nm, lead at 368 nm and silver at 328 nm provide specific signatures outside the normal waveband region of interest, but potentially useful for detection of, say, silver wire accelerated burning.

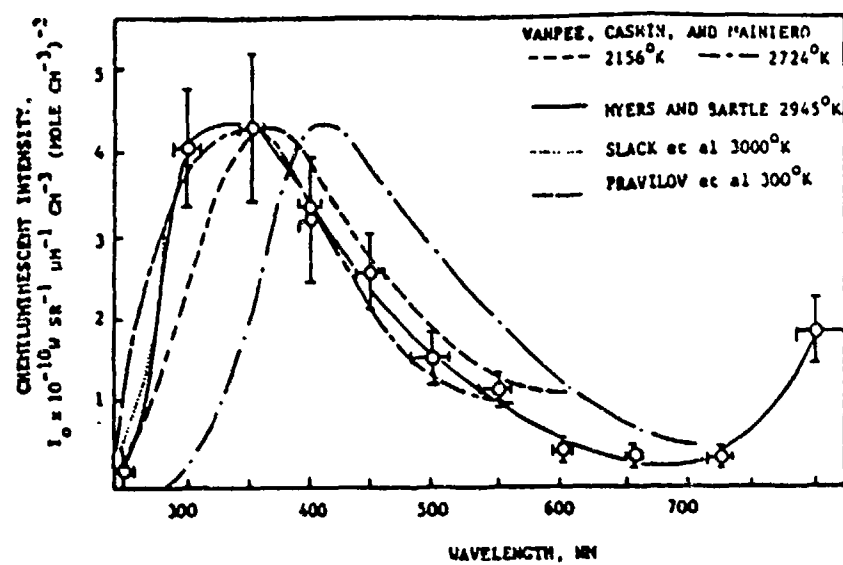


Figure 8: CO + O Chemiluminescent Intensity Spectra. The points with indicated errors bars as well as the solid line are the absolute intensity measurements of Myers and Bartle. The other curves were normalised to the peak intensity.

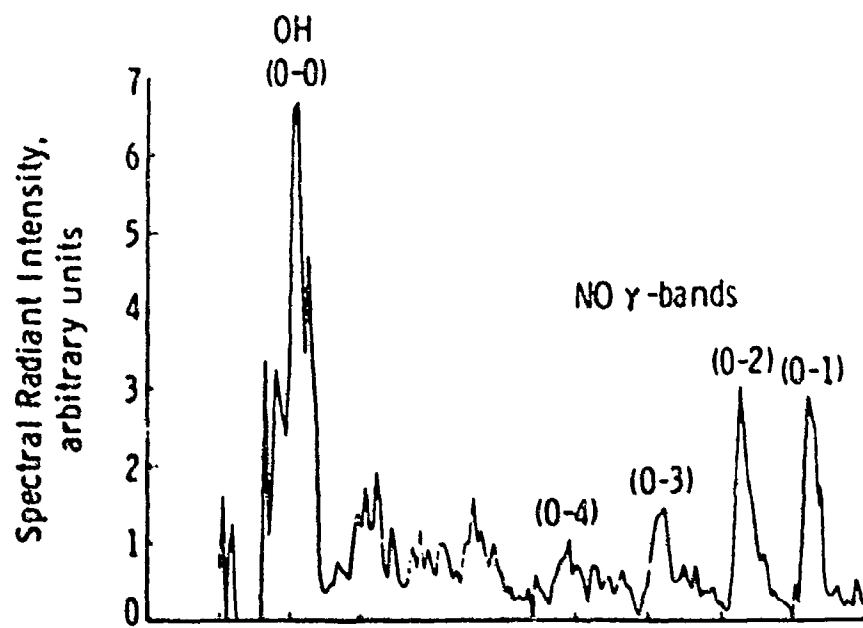


Figure 9: UV spectrum of plume showing band emissions.

4. Summary

Rocket motor plumes emit significant levels of radiation in the 270 to 290 nm ultraviolet transmission window between the ozone absorption band of the atmosphere and the shortest wavelength daylight background of solar radiation. This signal consists of continua from both thermally and chemically excited particulates and CO/O reaction chemiluminescence, and molecular emission bands from several species dominated by that of hydroxyl.

Radiation contributions from these and other sources can be computed from full knowledge of the chemical composition of the propellant, motor and atmosphere, the combustion reaction mechanism, and a precise flow field model, from which spatial distributions of particle sizes and temperatures and species concentrations together with the spectral data of those emitters and absorbers yield total radiation emission. Refinements of the data and extensions of the codes to include further details of trace species, and mechanisms not previously included, will often be required because the normally low ultraviolet signal results from minor components of the system and is therefore sensitively dependent on some apparently minor changes.

5. References

1. Hewish, M., Robinson, A. and Turbé, G.
"Airborne missile-approach warning"
Defense Electronics & Computing (Supplement to IDR 5/1991)
45-50 (1991)
2. Lewis R. Koller
"Ultraviolet Radiation"
(John Wiley & Sons, New York, 1965)
3. Huffman, R. E.
"Atmospheric Ultraviolet Remote Sensing"
(Academic Press, Boston, 1992)
4. Green, A. E. S. (Editor)
"The Middle Ultraviolet, Its Science and Technology"
(John Wiley & Sons, New York, 1966)
5. Patterson, E. M. and Gillespie, J. B.
"Simplified ultraviolet and visible wavelength atmosphere propagation model", Appl. Opt. 28(3), 425-429 (1989)
6. Trakhovsky, E., Ben-Shalom, A., Oppenheim, U. P., Devir, A. D., Balfour, L. S. and Engel, M.
"Contribution of oxygen to attenuation in the solar blind UV spectral region" Appl. Opt. 28(8), 1588-1591 (1989)

7. Trakhovsky, E.
"Ozone amount determined by transmittance measurements in the solar-blind ultraviolet spectral region" *Appl. Opt.* 24(21), 3519-3522 (1985)
8. Trakhovsky, E., Ben-Shalom, A. and Devir, A. D.
"Measurements of tropospheric attenuation in the solar blind UV spectral region and comparison with LOWTRAN-7 code" *SPIE Vol.1158 Ultraviolet Technology III* (1989)
9. World Meteorological Organization, Global Ozone Research and Monitoring Project - Report No. 16
"Atmospheric Ozone 1985" (NASA, 1985)
10. Finlayson-Pitts, B. J., Livingston, F. E. and Berko, H. N.
"Ozone destruction and bromine photochemistry at ground level in the Arctic spring" *Nature*, 343,622-625 (1990)
11. Johnson, R. P., Edwards, M. F. and Aldersey, A. L. H.
"A method for calculating ozone depth using the solar ultraviolet Fraunhofer spectrum" *J. Mod. Opt.* 34(8), 1031-1043 (1987)
12. Logan, J. A.
"Tropospheric Ozone: Seasonal Behaviour, Trends, and Anthropogenic Influence" *J. Geophys. Res.* 90(D6), 10463-10482 (1985)
13. Oltmans, S. J. and Komhyr, W. D.
"Surface Ozone Distributions and Variations From 1973-1984 Measurements at the NOAA Geophysical Monitoring for Climatic Baseline Observatories" *J. Geophys. Res.* 91(D4), 5229-5236 (1986)
14. Hough, A. M. and Derwent, R. G.
"Changes in the global concentration of tropospheric ozone due to human activities" *Nature*, 344, 645-648 (1990)
15. Kirchhoff, V. W. J. H.
"Ozone measurements in the troposphere of an Amazonian rain forest environment", *J. Geophys. Res.* 93(D12), 15850-15860 (1988)
16. Low, P. S., Davies, T. D., Kelly, P. M. and Farmer, G.
"Trends in Surface Ozone at Hohenpeissenberg and Arkona" *J. Geophys. Res.* 95(D13), 22441-22453 (1990)
17. Janach, W. E.
"Surface Ozone: Trend Details, Seasonal Variations, and Interpretation" *J. Geophys. Res.* 94(D15), 18289-18295 (1989)
18. Driscoll, W. G. and Vaughan, W. (Editors)
"Handbook of Optics"
(McGraw-Hill, New York, 1978)

19. Kolb, C. E., Ryali, S. B. and Wormhoudt, J. C.
"The Chemical Physics of Ultraviolet Rocket Plume Signatures"
SPIE Vol.932 "Ultraviolet Technology II" 2-23 (1988)
20. Hasson, V. and Nicholls, R. W.
"Absolute spectral absorption measurements on molecular oxygen from
2640-1920Å: I Herzberg I (triplet -triplet) bands (2640-2430Å)"
J. Phys. B. Atom. Molec. Phys., 4, 1778-1788 (1971)
21. Hasson, V. and Nicholls, R. W.
"Absolute spectral absorption measurements on molecular oxygen from
2640-1920Å: II Continuum measurements 2430-1920Å"
J. Phys. B. Atom. Molec. Phys., 4, 1789-1797 (1971)
22. Exton, R. J.
"An Ultraviolet Video Technique for Visualization of Stack Plumes and for
Measuring Sulfur Dioxide Concentration and Effluent Velocity"
NASA TP-1014, 1977
23. Ashby, R. A.
"Flames: A Study in Molecular Spectroscopy"
J. Chem. Ed., 52(10), 632-637 (1975)
24. Mavrodineanu, R and Boiteux, H.
"Flame Spectroscopy"
(John Wiley and Sons, New York, 1965)
25. Yates, G. J., Wilke, M., King, N and Lumpkin, A.
"Ultraviolet imaging of hydrogen flames"
SPIE 932, 271-278 (1988)
26. Williams, S. D.
"A preliminary study on the use of the ultraviolet exhaust plumes of
ICBMs for launch detection"
M. Sc. Thesis, Air Force Institute of Technology
AFIT/GSO/ENP/86D-3 (1986)
27. Krider, E. P., Noggle, R. C., Uman, M. A. and Orville, R. E.
"Lightning and the Apollo 17 / Saturn V Exhaust Plume"
J. Spacecraft, 11(2), 72-75 (1974)
28. Keefer, D. R., Phillips, W. J. and Harwell, K. E.
"Photographic Spectroscopic Measurement of Ultraviolet Solid Rocket
Motor Plumes" University of Tennessee Space Institute,
US Naval Weapons Center Contract No. N60530-78-C-0020 (1980)
29. O'Donnell, R. M. and Sauer, L. W.
"Development of Ultra-Violet Plume Signature Prediction Code
(PRUV)" Proc. SPIE 1725, 113-124 (1991)

30. Lyons, R. B., Wormhoudt, J. and Kolb, C. E.
"Calculation of Visible Radiation from Missile Plumes"
AIAA Paper 81-1111, Palo Alto, Ca., June 1981
31. Slack, M. and Grillo, A.
"High Temperature Rate Coefficient Measurements of CO + O
Chemiluminescence"
Combust. Flame 59, 189-196 (1985)
32. Collins, D. F.
"Quantitative Image Analysis of UV Rocket Plumes and Laboratory
Images" SPIE Vol 932, Ultraviolet Technology II, 204-212 (1988)
33. Scott, H. E., Pipes, J.G., Roux, J. A., Weller, C. S. and Opal, C. B.
"Plume Radiation Measurements in a Space Simulation Chamber"
SPIE 156, 184-192 (1978)
34. Jensen, D. E. and Jones, G. A.
"Reaction Rate Coefficients for Flame Calculations"
Combust. Flame 32, 1-34 (1978)
35. Levin, D. A., Caveny, L. H. and Mann, D. M.
"Ultraviolet Emissions Quantified by Rocket Payloads"
SPIE 1764, Ultraviolet Technology IV, 388-399 (1992)

SECURITY CLASSIFICATION OF THIS PAGE

UNCLASSIFIED

REPORT NO.
DSTO-TR-0002

AR NO. 920 REPORT SECURITY CLASSIFICATION
AR-008-~~005~~ Unclassified

TITLE

Ultraviolet emission from rocket motor plumes

AUTHOR(S)
David Kilpin

CORPORATE AUTHOR
DSTO Aeronautical and Maritime Research Laboratory
GPO Box 4331
Melbourne Victoria 3001

REPORT DATE
June, 1994

TASK NO.

SPONSOR

FILE NO.
510/207/0102

REFERENCES

PAGES

35 22

CLASSIFICATION/LIMITATION REVIEW DATE

CLASSIFICATION/RELEASE AUTHORITY
Chief, Explosives Ordnance Division

SECONDARY DISTRIBUTION

Approved for public release

ANNOUNCEMENT

Announcement of this report is unlimited

KEYWORDS

Ultraviolet radiation
Rocket motor plumes

Atmospheric transmission
signatures

Ultraviolet signatures

ABSTRACT

Atmospheric limitations on the spectral region of the ultraviolet appropriate for detection of emissions from rocket motor plumes are considered. Origins of ultraviolet emission as spectral continua, bands and lines from the rocket motor exhaust flow and its atmospheric interaction are discussed. The contrast of infrared emissions arising mostly from major products and processes with ultraviolet emissions often resulting from trace constituents and minor pathways, indicates the more detailed knowledge of the rocket motor system required for modelling and prediction of ultraviolet signatures.

SECURITY CLASSIFICATION OF THIS PAGE

UNCLASSIFIED

Ultraviolet Emission from Rocket Motor Plumes

David Kilpin

(DSTO-TR-0002)

DISTRIBUTION LIST

Director, AMRL
Chief, Explosives Ordnance Division
Dr R.J. Spear
David Kilpin
AMRL Library - Maribyrnong

Chief Defence Scientist (for CDS, FASSP, ASSCM) 1 copy only

Director, ESRL

AMRL Library - Fishermens Bend

Head, Information Centre, Defence Intelligence Organisation

OIC Technical Reports Centre, Defence Central Library

Officer in Charge, Document Exchange Centre

8 copies

Air Force Scientific Adviser, Russell Offices

Scientific Adviser - Policy and Command

Senior Librarian, Main Library DSTOS

Librarian, DSD, Kingston ACT

Serials Section (M List), Deakin University Library, Deakin University, Geelong 3217

NAPOC QWG Engineer NBCD c/- DENCRS-A, HQ Engineer Centre, Liverpool

Military Area, NSW 2174 *

ABCRA, Russell Offices, Canberra ACT 2600

4 copies

Librarian, Australian Defence Force Academy

Head of Staff, British Defence Research and Supply Staff (Australia)

NASA Senior Scientific Representative in Australia

INSPEC: Acquisitions Section Institution of Electrical Engineers

Head Librarian, Australian Nuclear Science and Technology Organisation

Senior Librarian, Hargrave Library, Monash University

Library - Exchange Desk, National Institute of Standards and Technology, US

Acquisition Unit (DXC-EO/GO), British Library, Boston Spa, Wetherby, Yorkshire LS23 7BQ, England

Library, Chemical Abstracts Reference Service

Engineering Societies Library, US

Documents Librarian, The Center for Research Libraries, US

Army Scientific Adviser, Russell Offices - data sheet only

Navy Scientific Adviser - data sheet only

Director General Force Development (Land) - data sheet only

DASD, APW2-1-OA2, Anzac Park West, Canberra ACT - data sheet only

SO (Science), HQ 1 Division, Milpo, Enoggera, Qld 4057 - data sheet only

Librarian - AMRL Sydney - data sheet only

Counsellor, Defence Science, Embassy of Australia - data sheet only

Counsellor, Defence Science, Australian High Commission - data sheet only

Scientific Adviser to DSTC Malaysia, c/- Defence Adviser - data sheet only

Scientific Adviser to MRDC Thailand, c/- Defence Attaché - data sheet only